

Wood Composites Based on *In Situ* Modification of Poplar Veneers by PEG-[Bmim]Cl

Zuju Shu,* Mengya Xie, Jin Yu, Xinyue Zhang, Huanhuan Li, and Baoshan Gao

Due to the high viscosity of pure [Bmim]Cl, PEG was selected to be co-solvent to form the solvent system. The dissolution and plasticization ability of PEG-[Bmim]Cl to poplar veneer was completed with processes such as hot pressing and coagulation bath to achieve the *in-situ* modification of poplar veneers to develop an innovative wood composite, which are expected to be molded. At the same time, the effects of the solvent system on the properties of wood composites were studied. The results showed that both the [Bmim]Cl-treated group (B) and the PEG-treated group (C) had a certain degree of plasticity when compared with the untreated group (A). The PEG-[Bmim]Cl-treated group (D) had the greatest ductility. The main reason was that PEG and [Bmim]Cl synergistically *in situ* dissolve the components of the veneer, increasing the proportion of the matrix phase (dissolved part). The interface bonding between the matrix phase and the reinforced phase was enhanced and resulted in the best comprehensive mechanical properties. However, no other derivative reactions occurred in each group.

DOI: 10.15376/biores.18.4.6815-6826

Keywords: Poplar veneers; [Bmim]Cl; PEG; Modification; Wood composites

Contact information: School of Light and Textile Industries Engineering & Art, Anhui Agricultural University, Hefei, Anhui 230036 China; *Corresponding author: shuzuju@ahau.edu.cn

INTRODUCTION

Environmental deterioration and shortage of resources caused by non-renewable and non-biodegradable resources are increasing. While more attention is being paid to renewable wood, wood can only be moulded into simple shapes due to its rigid nature (Dong *et al.* 2020). To improve the plasticity of wood veneers and broaden their applications, water, furfuryl alcohol, ammonia, and ionic liquids (ILs) have been used to modify them (Herold and Pfriem 2013; Ou *et al.* 2014; Šprdlík *et al.* 2016). These methods can be improved to be more environmentally friendly and efficient. In earlier research, ILs were used for wood pretreatment as a “green solvent” (Shu *et al.* 2017). Wood is a renewable resource composed of three macromolecular chemical components—cellulose, hemicelluloses, and lignin (Croitoru and Roata 2021; Bisht *et al.* 2022; Jiang *et al.* 2022). Generally, wood veneers are often obtained by rotary cutting or sliced cutting. However, the veneers obtained by rotary cutting have lower porosity and higher density compared with the sliced veneers (Kamperidou *et al.* 2020). ILs are potential solvents for most carbohydrate and lignocellulosic biomass that are insoluble in conventional solvents due to strong hydrogen bonding (Xu *et al.* 2019; Rajan *et al.* 2022; Wei *et al.* 2022). However, the high viscosity of ILs hinders the dissolution of lignocellulose (Goshadrou and Lefsrud 2017).

To lower the viscosity of the solution, green co-solvents should be employed for pretreatment, dissolution, or extraction. A co-solvent can prove helpful in reducing the cost of solvent (Rodriguez *et al.* 2009; Nasirpour and Mousavi 2021). N, N-dimethylformamide (DMF) and dimethyl sulfoxide (DMSO) are effective co-solvents, but they have toxic effects (Clarke *et al.* 2018; Yang *et al.* 2014). Polyethylene glycol (PEG, molecular weight greater than 4000) can be used as solvent or additive in solvent extraction systems due to its biodegradability, low toxicity, and low cost, with relatively low melting points and very low volatility. PEG dissolves lignin, and it has been used to develop cleaner, more efficient pulp delignification. ILs are often used in many practical applications such as efficient catalysts, clean energy storage, and pollutant gas treatment (Wang *et al.* 2022). As an environmentally friendly reaction medium, PEG is often used to dissolve chemicals, catalysts, complex metal cations, and participate in redox chemistry (Hoffmann 2022). Both ILs and PEG are considered to be in the framework of green chemistry. Given the remarkable thermal stability and the very low volatility of both ILs and PEG, PEG-ILs may be promising solvents for pretreatment of lignocellulose, dissolution of lignocellulose, and fractionation of its biopolymers (Willauer *et al.* 2000; Nasirpour and Mousavi 2018).

Wood obtained from fast growing poplar is an important bio-renewable lignocellulose resource. Poplar veneers are rotary cut or planed wood slices with high yield. The effective use of the veneer resources will increase the added value of the poplar wood (Shu *et al.* 2017). [Bmim]Cl, 1-butyl-3-methylimidazolium chloride was used as a low-cost IL to dissolve wood, cellulose, and lignin. The addition of cosolvent PEG further reduced the viscosity of PEG-[Bmim]Cl solvent system and the cost of this new technology (Goshadrou and Lefsrud 2017). In this work, mild impregnation of poplar veneers in PEG-[Bmim]Cl solution was expected to induce softening and plasticization of wood components. Subsequent hot-pressing and coagulation technology promoted an even *in-situ* dissolution and regeneration. The final drying resulted in a new environmentally friendly wood composite to meet the sustainable requirements.

EXPERIMENTAL

Materials

As raw material, the hybrid poplar clones (*Populus × euramericana* (Dode) Guiner CL. ‘Zhonglin 46’) aged from 5 to 6 years were randomly collected from the agricultural garden at Anhui Agricultural University. The lumber pieces were air-dried after being peeled. Selected lumber pieces, free from flaws such as knots, holes, cracks, fungi, and insect damage, were rotary cut (YD-335, Jinhua Yidi Medical Equipment Co., Ltd., China) into veneers with 1.8 ± 0.1 mm thickness. 1-Butyl-3-Methyl Imidazolium Chloride ([Bmim]Cl) with a purity of 99.0% was purchased from Lanzhou Institute of Chemical Physics, Chinese Academy of Sciences, and used without further purification. PEG (6000) was purchased from Shanghai Macklin Biochemical Co., Ltd. Deionized water (DW) was manufactured in the laboratory at Anhui Agricultural University.

Fabrication of Novel Wood Composites

The experimental procedure was performed as described by Shu *et al.* (2017). Figure 1 illustrates the procedure used to develop the novel wood composites. The prepared veneers were selected randomly, cut into 30 mm × 25 mm samples, and dried to a constant weight at 60 °C. The [Bmim]Cl solvent system has a higher viscosity, and full

impregnation requires higher energy and longer time. PEG was introduced to form the solvent system PEG-[Bmim]Cl with reduced viscosity. Three groups of prepared veneers (30 mm × 25 mm) were impregnated with [Bmim]Cl (B), PEG (C), and 20 wt.% PEG-80 wt.% [Bmim]Cl (D), which were melted already in the electric vacuum drying oven (DZF-6050, Nanjing Tianhuang Machinery Co., Ltd, China) at 90 °C. The untreated control group was defined as A. During this infiltration process, the impregnation temperature was 90 °C, while the immersion time was 24 h to ensure uniform soaking.

Subsequent hot-pressing (R-3212 Hot Press, Wuhan Qien Science and Technology Development Co., Ltd, China) promoted the dissolution of cellulose or cellulose/lignin with the synergistic effect of heat, pressure, and solvent. The hot-pressed veneer exhibited plastic deformation without fracture.

Afterward, *in-situ* partially dissolved veneers were placed into DW at room temperature to replace IL during the coagulation bath. Finally, the *in situ* modified veneers were dried by hot-pressing at 6 MPa and 160 °C for 30 min, and the resulting wood composites had a densified structure and excellent mechanical robustness. This hot pressing process can not only dry the modified veneer, but also fix the shape of the veneer to prevent it from deforming.

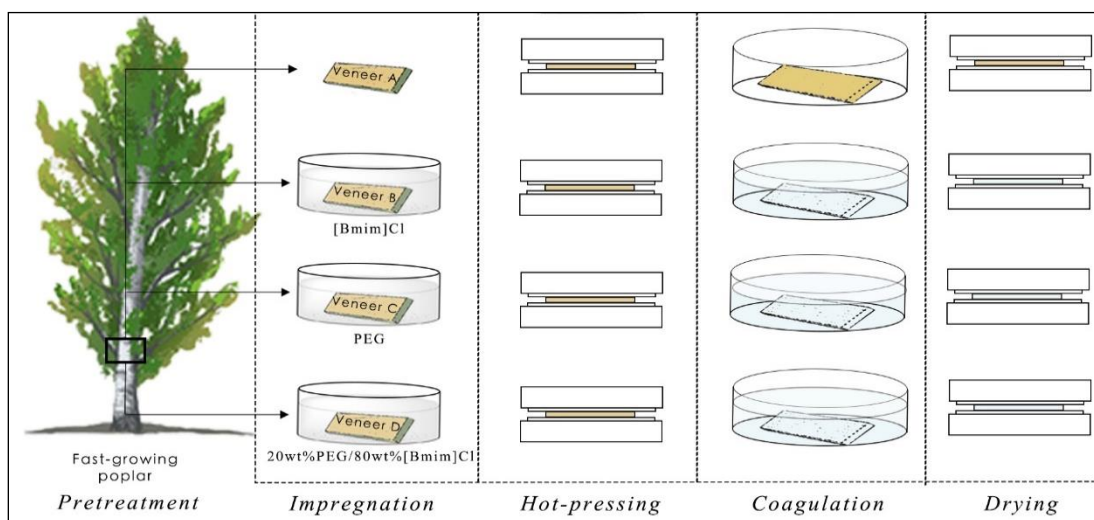


Fig. 1. Fabrication of novel wood composites

Scanning Electron Microscopy (SEM)

Scanning electron microscopy (S-48, Hitachi, Tokyo, Japan) was used to visualize the microstructure and evaluate the surface morphology of the novel wood composites. The samples were dried and sputter-coated with gold using an ion sputter coater (E1010, Hitachi) for 30 s with a current of 10 mA prior to observation. The surface topography of the samples was observed with a SEM using an accelerating voltage of 5 kV.

Tensile Test

The samples were cut into longitudinal samples with dimensions of 30 mm × 3 mm. 5 samples of each group were selected randomly. The mechanical properties were determined by the standard test method of ASTM D638 (2022), using the electronic universal material testing machine (AG-X plus, Shimadzu, Kyoto, Japan) at 25 °C and 50% relative humidity. The crosshead velocity was 10 mm/min (Khakalo *et al.* 2020).

Fourier Transform Infrared (FTIR) Spectrometry

The samples were also cut into longitudinal samples with dimensions of 30 mm × 3 mm. The attenuated total reflectance (ATR) mode of an FTIR Spectrometer (Tensor II, Bruker, Karlsruhe, Germany) was used to investigate the chemical components and their changes on the surface of samples without damage. The scanning resolution was 4 cm⁻¹. Both the background and sample scanning time were 32 s. The scanning wavelength ranged from 4000 to 400 cm⁻¹ (Khakalo *et al.* 2019).

X-ray Diffraction (XRD)

The samples were ball-milled after being frozen in liquid nitrogen, and the dried powder was used for XRD analysis. The powder XRD patterns for all samples were measured in reflection mode (CuK α radiation) on an X-ray diffractometer (XD-3, Beijing Purkinje General Instrument Co., Ltd, China) with a voltage of 36 kV and a current of 20 mA. Diffractograms were recorded in an angular range of 10° to 40° (2 θ) with a scanning speed 0.5°/min. According to the scanning pattern, the (002) diffraction peak was near 2 θ = 22°, whereas there was a minimum valley near 2 θ = 18°. The relative crystallinity index (CrI) was calculated according to the empirical formula of Segal *et al.* (1959),

$$CrI = \frac{I_{002} - I_{am}}{I_{002}} \times 100\% \quad (1)$$

where I_{002} is the intensity of the (002) diffraction angle (near 2 θ = 22°), I_{am} is for non-crystalline diffraction background scattering intensity (near 2 θ = 18°), and CrI is the relative crystallinity index.

RESULTS AND DISCUSSION

Morphology Analysis

Figure 2 shows that there were obvious macroscopic changes in 3 treated groups compared with group A. The increase of group D in width direction was the most evident, which indicated PEG could reduce the viscosity of the solvent system. The carrier [Bmim]Cl improved the swelling of lignocellulose during impregnation. During hot-pressing, [Bmim]Cl and PEG enhanced the plasticity of lignocellulose and promoted the dissolution of the veneer components under the synergistic effect of temperature, pressure, and time. For group C, PEG swelled the veneers during impregnation and only partially dissolved lignin during hot pressing. For group B, high viscosity led to limited penetration during impregnation and uneven dissolution during hot-pressing. The plasticity of group B treated by [Bmim]Cl was higher than the one treated by PEG, whereas the combination of PEG and [Bmim]Cl for group D resulted in the best ductility.

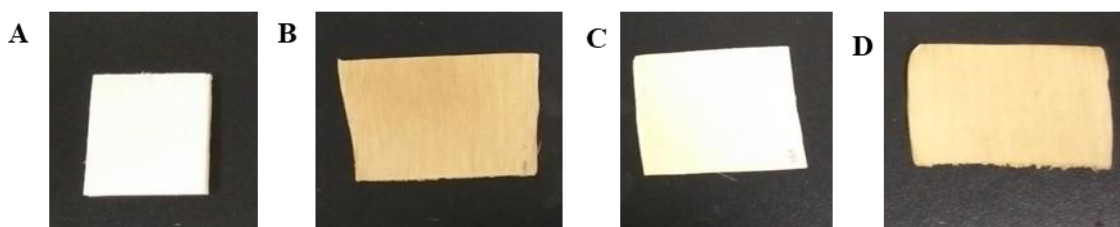


Fig. 2. Photos of samples

SEM images of each group (Fig. 3) showed that both [Bmim]Cl and PEG enhanced the plasticity of the veneers. For PEG treatment group (C), PEG swelled the veneers during impregnation and partially dissolved lignin during hot pressing to improve its anisotropy. The porous structure was densified by molding and shaping of the liquefied part. During impregnation and hot pressing, the ILs in Group B and D partially dissolved lignin and cellulose in wood. At the same time, hot pressing, with the synergy of temperature, pressure, and time, made the veneer easy to deform, which greatly improved its ductility. Among them, the veneers were not plasticized enough by [Bmim]Cl. When PEG was added to [Bmim]Cl to promote the dissolution of the wood components, the ductility of the sample was more obvious under the hot-press. Through molding, the reorganized veneer structure during the coagulation bath was fixed to make it denser, which improved the morphology and mechanical properties (Abushammala and Mao 2020).

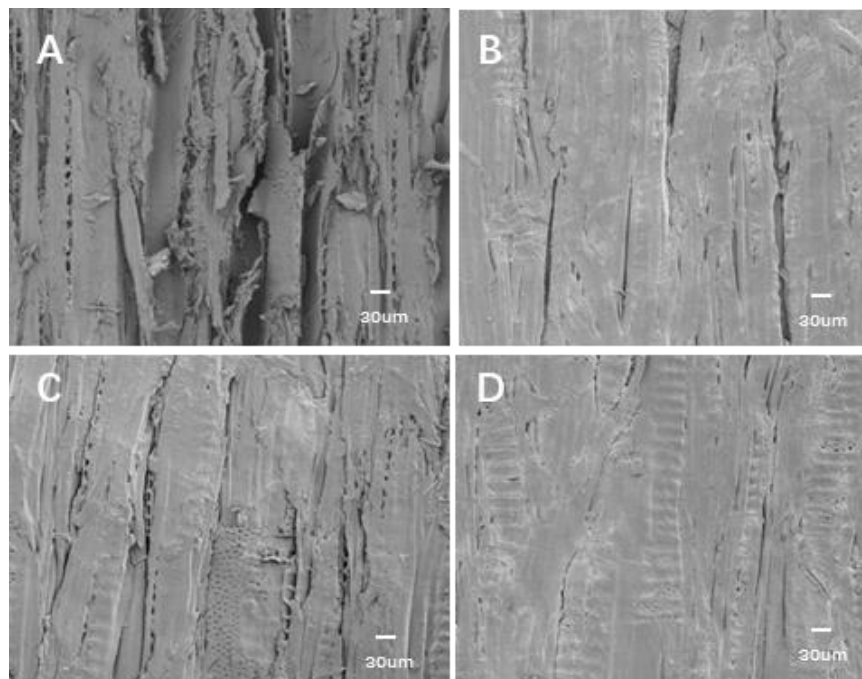


Fig. 3. SEM images of untreated wood (A) and *in situ* modified wood composites (B: the [Bmim]Cl-treated group; C: the PEG-treated group; D: The PEG-[Bmim]Cl-treated group)

Mechanical Properties

The mechanical properties of wood are determined by the properties of cell walls. Wood is a natural porous material that is formed by a large number of capillary systems of different scales in series or parallel. High porosity provides natural channels for the modification treatment of poplar wood. During impregnation, PEG or [Bmim]Cl was absorbed by veneer surfaces and gradually diffused. Under hot-pressing, PEG and [Bmim]Cl penetrated the cell wall to dissolve its components, which are then regenerated and reorganized into more compact structures (Croitoru and Roata 2020). Previous research has shown that [Bmim]Cl improves the material properties and plastic deformation, and the modified poplar veneers tend to be isotropic (Shu *et al.* 2017; Neyses *et al.* 2021). PEG produced the same result. The thickness, density, and longitudinal mechanical properties are shown in Table 1.

The tensile strength (TS) of Group D with the PEG-[Bmim]Cl solvent was the highest. There was almost no difference of elongation at break (EAB) and initial elastic modulus (E_0) among B, C, and D. By partially dissolving the components, each treatment promoted the regeneration and reorganization of the components. The control group (A) had the lowest TS, EAB, and E_0 . While the mechanical properties of three treated groups were improved, Group D had the best comprehensive mechanical properties. This result showed that PEG and [Bmim]Cl synergistically dissolved the components in the veneer, increasing the percentage of matrix phase, and the interfacial bonding between matrix phase and reinforcement phase was also enhanced (Acosta *et al.* 2020).

Table 1. Mechanical Properties of Untreated Wood (A) and *in situ* Modified Wood Composites (B: the [Bmim]Cl-treated group; C: the PEG-treated group; D: The PEG-[Bmim]Cl-treated group)

No.	t (mm)	ρ (g/cm ³)	TS (MPa)	EAB (%)	E_0 (GPa)
A	1.20(±0.03)	0.75(±0.16)	95.5(±14.2)	8.6(±3.0)	3.3(±0.5)
B	0.56(±0.07)	1.11(±0.53)	136.5(±9.9)	10.1(±2.6)	6.2(±0.7)
C	0.71(±0.07)	1.13(±0.08)	108.4(±17.6)	10.5(±0.4)	5.8(±0.5)
D	0.47(±0.01)	1.21(±0.29)	148.1(±23.3)	9.3(±0.8)	6.1(±0.8)

FTIR Analysis

The FTIR spectrum of each group is shown in Fig. 4. All FTIR spectra were similar, exhibiting the main peaks of lignocellulosic materials. It can be concluded that there were no other derivatization reactions during the treatment, and the components of poplar veneer were changed only in the proportions of cellulose, hemicellulose, and lignin. Therefore, the intensity of some corresponding absorbance peaks was different (Xiong *et al.* 2015)

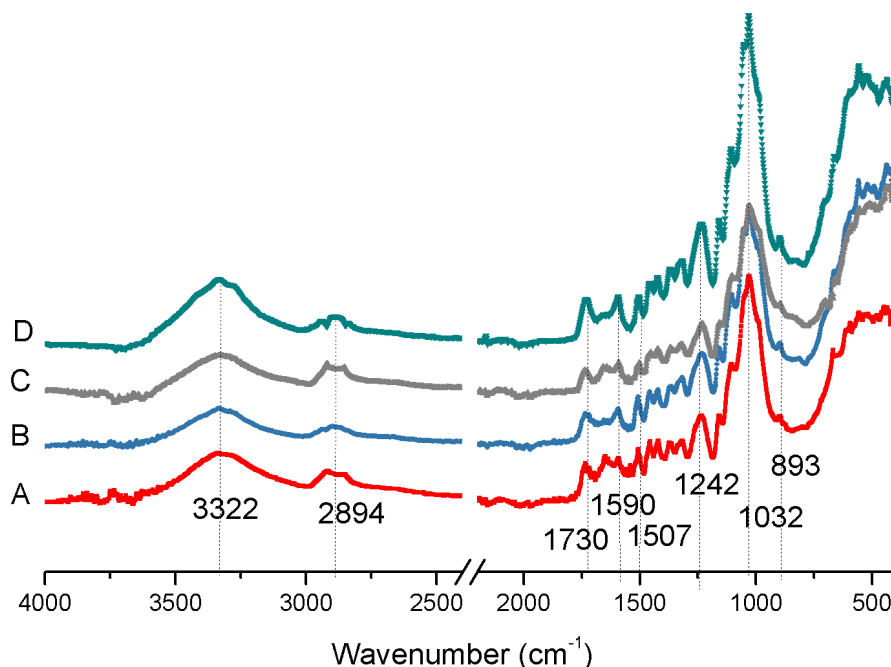


Fig. 4. ATR-FTIR spectra of untreated wood (A) and *in situ* modified wood composites (B: the [Bmim]Cl-treated group; C: the PEG-treated group; D: The PEG-[Bmim]Cl-treated group)

For Group B, the dissolved components were regenerated and reorganized in the coagulation bath. Although the intermolecular hydrogen bonds were not completely restored after recombination, they were rarely lost overall. Compared with the control group (A), the position and intensity of the absorbance band were not significantly different. At the same time, there was no characteristic peak of IL in group B, indicating that the ionic liquid was replaced in the coagulation bath.

For Group C, there were no characteristic peaks of PEG at 2900 cm^{-1} , 1330 cm^{-1} , and 1460 cm^{-1} , which may be due to substitution during the coagulation bath (Hu *et al.* 2013). For Group D, even if a small amount of PEG remained, high temperature may cause decomposition. Because lignin can be quickly degraded in alcohol, PEG cooperates with IL to destroy the lignin that wraps cellulose faster. The characteristic peaks of lignin at 1590 and 1507 cm^{-1} were weakened. However, the cellulose dissolved in the process of impregnation and hot pressing can be regenerated. Thus, there was an obvious characteristic absorbance peak of cellulose (Xie *et al.* 2012).

XRD Analysis

In Fig. 5, the (002) crystal planes of groups A, B, C, and D were located at 21.97° , 21.73° , 21.77° , and 21.70° , and their (001) crystal planes were located at 15.82° , 15.23° , 15.01° , and 15.16° , respectively. The (002) and (001) plane of each group had a very slight offset to the left, which remained in the vicinity of $2\theta=22^\circ$ and $2\theta=15^\circ$, and the interlayer spacing of crystal planes among each group had almost no change, which indicated each treatment had no effect on its crystalline region. Each group had a trough near $2\theta=18^\circ$, which was the maximum value of the scattering intensity of the amorphous region. So the crystal structure of the modified group was still the same as the control group.

Through calculation, CrI of each group was 67.0%, 73.4%, 73.0%, and 72.8%, respectively. The CrI of the wood composites of Group B, C, and D increased, and there was almost no difference. To a certain extent, CrI can reflect the physical and chemical properties of plant biomass materials, and it was an important basis for evaluating the mechanical properties. Generally, the tensile strength and other mechanical properties of lignocellulosic materials increase with higher CrI (Oosthuizen *et al.* 2023). The CrI corresponded to the tensile strength in Table 1.

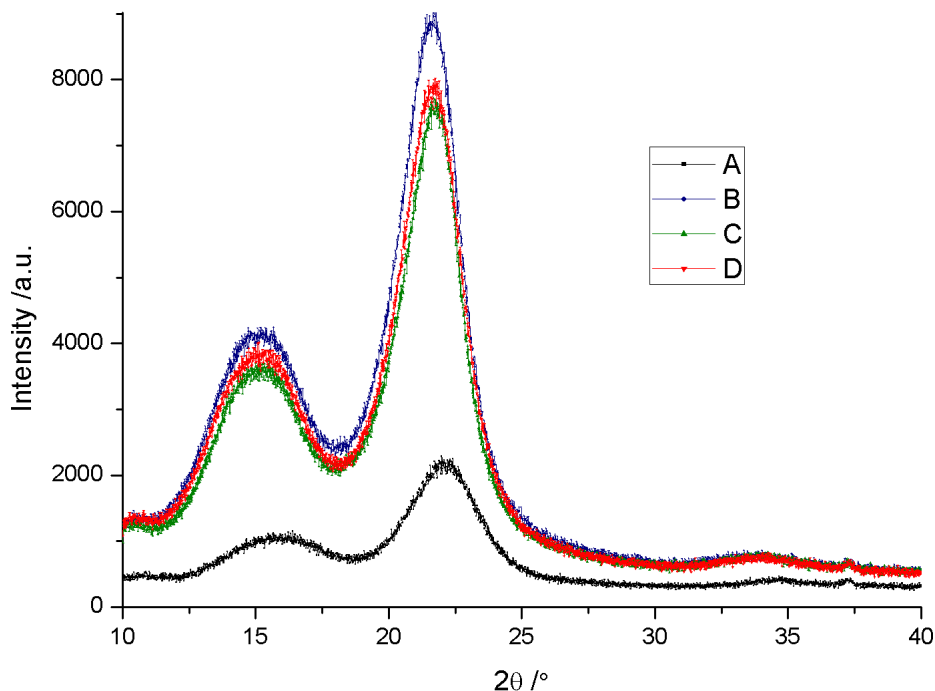


Fig. 5. XRD spectra of untreated wood (A) and *in situ* modified wood composites (B: the [Bmim]Cl-treated group; C: the PEG-treated group; D: The PEG-[Bmim]Cl-treated group)

For Group B, [Bmim]Cl fully wetted the veneer under the temperature of 90 °C, and very few components were dissolved during impregnation. When hot-pressed under the temperature of 160 °C, more lignin and carbohydrates were dissolved by [Bmim]Cl. At the same time, the increased fluidity of the cellulose chain promoted the reorganization of the amorphous region of cellulose. In the coagulation bath, the dissolved part was regenerated and reorganized. However, the dissolved hemicellulose was lost in the coagulation bath, which led to an increase in CrI, reaching 73.4%.

PEG can penetrate the wood cell wall and act as a swelling agent, leaving the cell wall in a permanent swelling state and no longer shrinking. The cellulose also swelled, which mainly included two types: swelling in the intra crystallization region and swelling in the inter crystallization region. When the swelling agent only penetrated the amorphous region, swelling of the intercrystalline region occurred, and the XRD pattern remained unchanged with the peak intensity changed. When the swelling agent can penetrate the amorphous and crystalline regions, swelling in the intra crystallization region occurred (Xu 2012). From Figure 4, only the swelling of the intercrystalline region occurred in each treatment group. For Group C, PEG can enter the amorphous region of cellulose, causing the amorphous region to swell. PEG itself was partly crystalline with a certain degree of crystallinity. Without protection of IL, even a small amount of retained PEG was to be thermally decomposed into smaller molecules under the high temperature. Therefore, the amorphous area was degraded without affecting the compact crystalline area, resulting in an increase in crystallinity and no characteristic peaks of PEG ($2\theta=19^\circ$ and 23°).

For the PEG-[Bmim]Cl-treated group, the veneers were easily dissolved because of the different solubility between PEG and [Bmim]Cl (Rodriguez *et al.* 2009). During the coagulation bath, PEG or [Bmim]Cl were replaced. Thus, the peak intensity of C and D spectra in Fig. 5 changed, but there was no characteristic diffraction peak of PEG (Meints *et al.* 2018).

CONCLUSIONS

1. Using poplar veneers as the raw material and [Bmim]Cl, PEG, or PEG-[Bmim]Cl as the solvent system, novel wood composites were developed through a series of impregnation, hot pressing, coagulation bath, and drying. The solvent can be effectively replaced in the coagulation bath to obtain all-wood composite materials with plasticity, which provides a basis for the molding of wood.
2. The macroscopic and microstructures of each treatment group showed that: [Bmim]Cl, PEG or PEG-[Bmim]Cl all made the veneers swell and enhance their plasticity and ductility. The synergistic effect of immersing in the solvent system and hot pressing facilitated the wood components to dissolve and flow. After the coagulation bath, the dissolved part reorganized. Thus, the modified veneers tended to be uniform in all directions. Group D had the best ductility with the biggest macroscopic dimensional change. PEG as a co-solvent can help dissolve the veneers, and the veneers' plasticity and ductility can be improved by the synergistic effect of PEG and [Bmim]Cl.
3. The tensile strength (TS), elongation at break (EAB), and initial elastic modulus (E_0) of each treatment group were higher than that of untreated one. These results indicated that the partial dissolution of the components by the solvent system can promote the recombination of the components during the coagulation bath process, thereby improving the mechanical properties and plasticity of the veneers. Group D had the best overall mechanical properties, which was attributed to synergistic solubility of PEG and [Bmim] Cl, increasing the percentage of matrix phase. The interface bonding between the matrix phase and the reinforcement phase was enhanced, thereby improving its comprehensive mechanical properties.
4. The relative crystallinity of group B (73.4%) was the highest. Group A (67.0%) was the lowest. The relative crystallinity was consistent with the mechanical properties. No characteristic Fourier transform infrared (FTIR) peaks of PEG were found in Groups C and D, indicating that no other derivatization reactions occurred in each treatment. Only some of the absorbance peaks were different in intensity. Both from X-ray diffraction (XRD) and FTIR, the composition of poplar veneer was not changed, only the ratio of cellulose, hemicellulose, and lignin changed.

ACKNOWLEDGMENTS

The authors are grateful for the support of Anhui Natural Science Foundation (2018085MC84), the College Students Innovation and Entrepreneurship Training Program (X202210364429, X202210364678, X202210364485).

REFERENCES CITED

- Abushammala, H., and Mao, J. (2020). "A review on the partial and complete dissolution and fractionation of wood and lignocelluloses using imidazolium ionic liquids," *Polymers* 12(1), 195-223. DOI: 10.3390/polym12010195

- Acosta, A. P., Labidi, J., Schulz, H. R., Gallio, E., Barbosa, K.T., Beltrame, R., de Avila Delucis, R., and Gatto, D. A. (2020). "Thermochemical and mechanical properties of pine wood treated by in situ polymerization of methyl methacrylate (MMA)," *Forests* 11(7), 768-777. DOI: 10.3390/f11070768
- Bisht, P., Pandey, K. K., and Srinivas, G. (2022). "Physiochemical characterization and thermal behaviour of transparent wood composite," *Materials Today Communications* 31, article 103767. DOI: 10.1016/j.mtcomm.2022.103767
- Clarke, C. J., Tu, W. C., Levers, O., Bröhl, A., and Hallett, J. P. (2018). "Green and sustainable solvents in chemical processes," *Chemical Reviews* 118(2), 747-800. DOI: 10.1021/acs.chemrev.7b00571
- Croitoru, C., and Roata, I. C. (2020). "Ionic liquids as antifungal agents for wood preservation," *Molecules* 25(18), article 4289. DOI: 10.3390/molecules25184289
- Croitoru, C., and Roata, I. C. (2021). "Alkylimidazolium ionic liquids absorption and diffusion in wood," *Applied Sciences* 11(16), 7640-7648. DOI: 10.3390/app11167640
- Dong, Y. M., Wang, K. L., Li, J. Z., Zhang, S. F., and Shi, S. Q. (2020). "Environmentally benign wood modifications: A review," *ACS Sustainable Chemistry & Engineering* 8(9), 3532-3540. DOI: 10.1021/acssuschemeng.0c00342
- Goshadrou, A., and Lefsrud, M. (2017). "Synergistic surfactant-assisted [EMIM]OAc pretreatment of lignocellulosic waste for enhanced cellulose accessibility to cellulase," *Carbohydrate Polymers* 166, 104-113. DOI:10.1016/j.carbpol.2017.02.076
- Herold, N., and Pfriem, A. (2013). "Impregnation of veneer with furfuryl alcohol for an improved plasticization and moulding," *European Journal of Wood and Wood Products* 71, 281-282. DOI: 10.1007/s00107-013-0677-4
- Hoffmann, M. M. (2022). "Polyethylene glycol as a green chemical solvent," *Current Opinion in Colloid & Interface Science* 57. DOI: 10.1016/j.cocis.2021.101537
- Hu, X., Wang, J., and Huang, H. (2013). "Impacts of some macromolecules on the characteristics of hydrogels prepared from pineapple peel cellulose using ionic liquid," *Cellulose* 20, 2923-2933. DOI: 10.1007/s10570-013-0075-4
- Jiang, J., Wang, C., Ebrahimi, M., Shen, X. J., and Mei, C. T. (2022). "Eco-friendly preparation of high-quality mineralized wood via thermal modification induced silica sol penetration," *Industrial Crops and Products* 183, article 115003. DOI: 10.1016/j.indcrop.2022.115003
- Kamperidou, V., Aidinidis, E., and Barboutis, I. (2020). "Impact of structural defects on the surface quality of hardwood species sliced veneers," *Applied Sciences* 10(18), article 6265. DOI: 10.3390/app10186265
- Khakalo, A., Tanaka, A., Korpela, A., and Orelma, H. (2020). "Delignification and ionic liquid treatment of wood toward multifunctional high-performance structural materials," *ACS Applied Materials & Interfaces* 12(20), 23532-23542. DOI: 10.1021/acsami.0c02221
- Khakalo, A., Tanaka, A., Korpela, A., Hauru, L. K. J., and Orelma, H. (2019). "All-wood composite material by partial fiber surface dissolution with an ionic liquid," *ACS Sustainable Chemistry and Engineering* 7(3), 3195-3202. DOI: 10.1021/acssuschemeng.8b05059
- Meints, T., Hansmann, C., and Gindl-Altmatter, W. (2018). "Suitability of different variants of polyethylene glycol impregnation for the dimensional stabilization of oak wood," *Polymers* 10(1), 81. DOI: 10.3390/polym10010081
- Nasirpour, N., and Mousavi, S. M. (2018). "RSM based optimization of PEG assisted ionic liquid pretreatment of sugarcane bagasse for enhanced bioethanol production:

- Effect of process parameters,” *Biomass and Bioenergy* 116, 89-98. DOI: 10.1016/j.biombioe.2018.06.008
- Nasirpour, N., and Mousavi, S.M. (2021). “Effect of particle size in polyethyltene glycol-assisted [BMIM][Cl] pretreatment of sugarcane bagasse,” *Bioenergy Research* 14(4), 1136-1146. DOI: 10.1007/s12155-020-10237-1
- Neyses, B., Peeters, K., Buck, D., Rautkari, L., and Sandberg, D. (2021). “*In situ* penetration of ionic liquids during surface densification of Scots pine,” *Holzforschung* 75(6), 555-562. DOI: 10.1515/hf-2020-0146
- Oosthuizen, H., du Toit, E. L., Loots, M. T., Atanasova, M., Wesley-Smith, J., Crous, S., Weldhagen, M., and Focke, W. W. (2023). “A novel cost-effective choline chloride/ionic liquid solvent for all-cellulose composite production,” *Cellulose* 30, 127-140. DOI: 10.1007/s10570-022-04907-w
- Ou, R. X., Xie, Y. J., Wang, Q. W., Sui, S. J., and Wolcott, M. P. (2014). “Thermoplastic deformation of poplar wood plasticized by ionic liquids measured by a nonisothermal compression technique,” *Holzforschung* 68(5), 555-566. DOI: 10.1515/hf-2013-0136
- Rajan, K., Kim, K., Elder, T. J., Naskar, A. K., and Labbé, N. (2022). “Ionic-liquid-assisted fabrication of lignocellulosic thin films with tunable hydrophobicity,” *ACS Sustainable Chemistry & Engineering* 10 (27), 8835-8845. DOI: 10.1021/acssuschemeng.2c01741
- Rodriguez, H., Francisco M., Rahman M., Sun N., and Rogers R. D. (2009). “Biphasic liquid mixtures of ionic liquids and polyethylene glycols,” *Physical Chemistry Chemical Physics* 11(46), 10916-10922. DOI: 10.1039/b916990c
- Segal, L., Creely, J. J., Martin, A. E., and Conrad, C.M. (1959). “An empirical method for estimating the degree of crystallinity of native cellulose using the Xray diffractometer,” *Textile Research Journal* 29(10), 786-794. DOI: 10.1177/004051755902901003
- Shu, Z. J., Liu, S. Q., Zhou, L., Li, R., Qian, L. C., Wang, Y. N., Wang, J. J., and Huang, X. H. (2017). “Physical and mechanical properties of modified poplar veneers,” *BioResources* 12(1), 2004-2014. DOI: 10.15376/biores.12.1.2004-2014
- Šprdlík, V., Brabec, M., Mihailović, S., and Rademacher, P. (2016). “Plasticity increase of beech veneer by steaming and gaseous ammonia treatment,” *Maderas-Ciencia y Tecnología* 18(1), 91-98. DOI: 10.4067/s0718-221x2016005000009
- Wang, Y., Lu, Y., Wang, C., Zhang, Y., Huo, F., He, H., and Zhang, S. (2022). “Two-dimensional ionic liquids with an anomalous stepwise melting process and ultrahigh CO₂ adsorption capacity,” *Cell Reports Physical Science* 3(7). DOI: 10.1016/J.XCRP.2022.100979
- Wei, J., Gao, H. S., Li, Y., and Nie, Y. (2022). “Research on the degradation behaviors of wood pulp cellulose in ionic liquids,” *Journal of Molecular Liquids* 356, article 119071. DOI: 10.1016/j.molliq.2022.119071
- Willauer, H. D., Huddleston, J. G., Li, M., and Rogers, R. D. (2000). “Investigation of aqueous biphasic systems for the separation of lignins from cellulose in the paper pulping process,” *Journal of Chromatography B* 743, 127-135. DOI: 10.1016/s0378-4347(00)00222-x
- Xie, C., Liu, Z. M., Wu, P., Wang, H. Y., and Meng, W. (2012). “Preparation and characterization of polyethylene glycol wood composite phase change materials,” *Scientia Silvae Sinicae* 48(9), 120-126. DOI: 10.11707/j.1001-7488.20120919
- Xiong, F., Zhou, L., Qian, L., and Liu, S. (2015). “Effects of pretreatment methods using various 1,4-dioxane concentrations on the performance of lignocellulosic films

of *Eucalyptus citriodora*,” *BioResources* 10(1), 1149-1161. DOI:
10.15376/biores.10.1.1149-1161

Xu, F., Chen, Y. L., You, T. T., Mao, J. Z., and Zhang, X. (2019). “Research progress on mechanism of cellulose dissolution,” *Journal of Forestry Engineering* 4(1), 1-7. DOI: 10.13360/j.issn.2096-1359.2019.01.001

Xu, W. Y. (2012). *Properties and Characterization of Polyethylene Glycol/Heat Treated Poplar*, Master’s Thesis, Beijing Forestry University, Beijing, China.

Yang, N., Chen, X., Lin, F., Ding, Y., Zhao, J., and Chen, S. (2014). “Toxicity formation and distribution in activated sludge during treatment of N, N-dimethylformamide (DMF) wastewater,” *Journal of Hazardous Materials* 264, 278-285. DOI: 10.1016/j.jhazmat.2013.10.002

Article submitted: May 17, 2023; Peer review completed: June 3, 2023; Revised version received and accepted: June 28, 2023; Published: August 7, 2023.

DOI: 10.15376/biores.18.4.6815-6826